ROBUST REFLECTIVE BEAMFORMING FOR NON-TERRESTRIAL NETWORKS UNDER THERMAL DEFORMATIONS

Damir Rakhimov, Bile Peng†, Eduard Jorswieck†, Martin Haardt**

* Communications Research Laboratory, Ilmenau University of Technology, Germany
Emails: {damir.rakhimov, martin.haardt}@tu-ilmenau.de
† Institute for Communications Technology, Technical University of Braunschweig, Germany
Emails: {b.peng, e.jorswieck}@tu-bs.de

ABSTRACT

In this paper, we present a beamforming method that is robust against thermal deformations for non-terrestrial reconfigurable intelligent surfaces (RIS). We analytically derive the expressions for the worst-case bound on perturbations of the covariance matrix and the corresponding steering vectors as functions of possible displacements of RIS elements. We apply these bounds during the optimization procedure to find the beamforming coefficients that are robust to thermal deformations. Moreover, we present a simple heuristic to obtain the constant modulus beamforming coefficients from the optimal beamforming via an array thinning operation. The simulation results confirm the robustness of the proposed solution against random but bounded perturbations caused by thermal deformations of the reflective surface.

1. INTRODUCTION

The topic of non-terrestrial RIS-assisted communications [1, 2] recently attracted extensive attention from the research community as a promising technique to extend the functionality of antenna systems at satellites [3–6]. While the cost of the deployment of active phase arrays in space might be high, the usage of light-weight and low-cost metamaterials with the additional possibility to adjust its parameters in real-time directly in orbit looks like an appealing solution to enable beamforming.

However, the deployment of large antenna systems in space is related to a number of challenges that complicate the design and the implementation of such systems in practice. The deformations of any large surface deployed in space [7] is one such factor. There might be different reasons for such deformations but it mainly occurs due to uneven spreading of temperature over the surface during operation because different parts of a satellite are exposed to a varying amount of sunlight which make them expand or shrink at different degrees. As a result, the change of curvature influences the antenna directivity and the level of the sidelobes [8].

Due to the potentially large size and higher operational frequency, it is very likely that one of the sides of the communication link will be located in the radiative near-field [9] which should be taken into account during the analysis and the design of the corresponding algorithms. The authors in [10, 11] analyze the performance of RISs in the near-field and derive the power scaling law for RISs assuming extremely large surfaces and the associated near-field effects.

However, as an initial contribution to the topic of robust reflective beamforming against geometry deformation, we assume that both sides of the communication link are located in the far field. The original goal is the investigation of methods to reduce the sensitivity to practical impairments rather than achieve the best possible performance by placing the reflective structure in the radiative near-field. Further, we show that this simplification allows us to derive an analytical expression on the bounds of the perturbations of the covariance matrix and the array steering vectors. Nevertheless, we see the extension to the case of the radiative near field as a potential direction for follow-up research investigations.

Additionally, for this report, we limit ourselves to only linear geometries of reflecting apertures to derive the initial results that can also be extended to planar and arbitrary geometries of RISs. For convenience, we refer to such devices as reflecting line arrays (RLAs). Similarly to RISs, we can control the phase of the reflected signal at each element of an RLA thus implementing the reflective beamforming. We assume that an RLA is a passive device in the sense that it has no ability to process signals and requires external control for operation. We also assume that the cell of an RLA can be configured to absorb or reflect the impinging signal. For the impinging signal, we can only control the phase of the reflection coefficients. In this work, we ignore the reflection losses, the dependency of the amplitude on the phase, and mutual coupling effects.

In this paper, we analyze the application of a reconfigurable intelligent surface for enabling adaptive beamforming under thermal deformations. To this end, we present robust reflective beamforming for non-terrestrial networks under thermal deformations. We derive bounds on norms of perturbations of the compounding steering vector and the matrix of the overall noise reflected by the RIS as a function of the bound on the coordinate displacements. These results facilitate the robust deployment of large-size low-cost antenna systems in space with high directivity and high antenna gains that will enable direct ground-to-space connectivity of conventional mobile phones and provide seamless coverage across all areas on Earth with a cellular connection and internet [12].

Notation: In our work, we use the following notation. We use a, $\boldsymbol{a}$, and $\boldsymbol{A}$ to represent a scalar, a vector, and a matrix, respectively. $\boldsymbol{A}^{\mathrm{T}}$, and $\boldsymbol{A}^{\mathrm{H}}$ are the matrix transpose and the conjugate transpose, respectively. Furthermore, z^* is the conjugate of a complex number, $|a|$ is the magnitude of a scalar, $\|\boldsymbol{a}\|_2$ represents the 2-norm, $\|\boldsymbol{A}\|_{\mathrm{F}}$ denotes the Frobenius norm. We use $\odot$ to denote the element wise (Hadamard) product. We refer to the (m, n) element of a matrix $\boldsymbol{A}$ via $\left[\boldsymbol{A}\right]_{m,n}$.

This work has been supported in part by the ESA under the project SatNEX-V WI Y2.1.

2. SYSTEM MODEL

We consider a SISO communication system that communicates via an RLA in the far field in space. Due to periodic exposure to sun and shadowing effects, the surface of such an RLA will experience a temperature gradient causing random deformations of the reflective aperture. We show how the information about the worst-case deformations might be taken into account during the design stage to improve the system performance in terms of the RLA directivity.

For simplicity, we assume that each element of the RLA has a unit gain and the corresponding effective aperture $A_{\mathrm{e}} = \frac{\lambda^2}{4\pi}$. However, generalizations are possible. We consider the orientation of the RLA along the x-axis and consisting of N_{cell} elements. We assume that the phase center of the RLA matches the origin of the coordinate system. The spacing between elements is denoted as Δ.

2.1. Signal model

Following [13] the received signal at the ground terminal after the reflection at the RLA can be written as

$$y = \sum_{n=0}^{N_{\mathrm{cell}}-1} \sqrt{P_{\mathrm{tx}}\beta} \mathrm{e}^{-j\varphi_n^{(\mathrm{rfl})}} \cdot \mathrm{e}^{j\varphi_n^{(\mathrm{rla})}} \cdot \mathrm{e}^{j\varphi_n^{(\mathrm{imp})}} \cdot s + z, \qquad (1)$$

which can also be rewritten in the vector form

$$y = \sqrt{P_{\mathrm{tx}}\beta}\, \boldsymbol{a}_{\mathrm{rfl}}^{\mathrm{H}}\, \boldsymbol{\Phi}\, \boldsymbol{a}_{\mathrm{imp}} s + z \in \mathbb{C}, \qquad (2)$$

where $\boldsymbol{a}_{\mathrm{imp}} \in \mathbb{C}^{N_{\mathrm{cell}} \times 1}$ is the steering vector comprising the responses between the transmitter and every cell of the RLA, $\boldsymbol{\Phi} \in \mathbb{C}^{N_{\mathrm{cell}} \times N_{\mathrm{cell}}}$ is a diagonal matrix consisting of the phase coefficients for RLA's elements, $\boldsymbol{a}_{\mathrm{rfl}} \in \mathbb{C}^{N_{\mathrm{cell}} \times 1}$ is the steering vector comprising the responses between the receiver and every element of the RLA, P_{tx} is the transmit power, z is a sample of the additive white Gaussian noise (AWGN), and β is the overall path gain. For simplicity, we assume $\beta = 1$.

Both steering vectors $\boldsymbol{a}_{\mathrm{imp}} \in \mathbb{C}^{N_{\mathrm{cell}} \times 1}$ and $\boldsymbol{a}_{\mathrm{rfl}} \in \mathbb{C}^{N_{\mathrm{cell}} \times 1}$ have an identical structure and can be defined as a function of the spatial direction μ in the following way

$$\boldsymbol{a}(\mu) = \mathrm{e}^{-j\left(\frac{M-1}{2}\right)\mu} \cdot \left[\, 1 \;\; \mathrm{e}^{j\mu} \;\; \cdots \;\; \mathrm{e}^{j(M-1)\mu} \,\right]^{\mathrm{T}}, \qquad (3)$$

where we define the spatial frequency as $\mu(\theta) = -\frac{2\pi}{\lambda}\Delta\sin(\theta)$, while θ is the angle towards the source or the user, respectively. For simplicity, we assume that each element of the RLA is isotropic and its complex response does not depend on the spatial frequency μ.

For the conventional reflective beamforming, the phase coefficients across the RLA can be found as the difference between the phases for the reflected and the impinging signals [14]

$$\varphi_n^{(\mathrm{rla})} = \varphi_n^{(\mathrm{rfl})} - \varphi_n^{(\mathrm{imp})} \in \mathbb{R}. \qquad (4)$$

2.2. Optimization function

The reflective beampattern of the RLA $F\left(\theta, \boldsymbol{\phi}; \theta_{\mathrm{tx}}\right)$ for the given elevation angle of interest θ and the vector of RLA phase coefficients $\boldsymbol{\phi}$, parametrized by the elevation angle of the source θ_{tx} in the far field can be found as

$$\begin{aligned} F\left(\theta, \boldsymbol{\phi}; \theta_{\mathrm{tx}}\right) &= \left| \left(\boldsymbol{\phi} \odot \boldsymbol{a}_{\mathrm{imp}}\left(\theta_{\mathrm{tx}}\right)\right)^{\mathrm{H}} \cdot \boldsymbol{a}(\theta) \right|^2 && (5) \\ &= \boldsymbol{\phi}^{\mathrm{H}} \left(\left(\boldsymbol{a}_{\mathrm{imp}}^* \odot \boldsymbol{a}\right) \left(\boldsymbol{a}_{\mathrm{imp}}^* \odot \boldsymbol{a}\right)^{\mathrm{H}} \right) \boldsymbol{\phi} && (6) \\ &= \boldsymbol{\phi}^{\mathrm{H}} \boldsymbol{a}_{\mathrm{c}} \boldsymbol{a}_{\mathrm{c}}^{\mathrm{H}} \boldsymbol{\phi}, && (7) \end{aligned}$$

where we introduce a new variable to shorten the notation $\boldsymbol{a}_{\mathrm{c}} = \boldsymbol{a}_{\mathrm{imp}}^* \odot \boldsymbol{a}$. We drop the dependency on the angles to simplify the notation.

The corresponding directivity of an RLA can be defined as

$$D\left(\theta; \theta_{\mathrm{tx}}, \boldsymbol{\phi}\right) = 4\pi \frac{F\left(\theta; \theta_{\mathrm{tx}}, \boldsymbol{\phi}\right)}{\int_0^{\pi} F\left(\theta; \theta_{\mathrm{tx}}, \boldsymbol{\phi}\right) \sin(\theta)\, d\theta}. \qquad (8)$$

Similarly to [15], we can rewrite it in the matrix form as

$$D\left(\theta; \theta_{\mathrm{tx}}, \boldsymbol{\phi}\right) = \frac{\boldsymbol{\phi}^{\mathrm{H}} \boldsymbol{A}(\theta; \theta_{\mathrm{tx}}) \boldsymbol{\phi}}{\boldsymbol{\phi}^{\mathrm{H}} \boldsymbol{B}(\theta_{\mathrm{tx}}) \boldsymbol{\phi}}, \qquad (9)$$

where

$$\begin{aligned} \boldsymbol{A}(\theta; \theta_{\mathrm{tx}}) &= \boldsymbol{a}_{\mathrm{imp}}^* \boldsymbol{a}_{\mathrm{imp}}^{\mathrm{T}} \odot \boldsymbol{a}\boldsymbol{a}^{\mathrm{H}}, && (10) \\ \boldsymbol{B}(\theta_{\mathrm{tx}}) &= \frac{1}{2} \int_{-\pi/2}^{\pi/2} \left(\boldsymbol{a}_{\mathrm{imp}}^* \boldsymbol{a}_{\mathrm{imp}}^{\mathrm{T}} \odot \boldsymbol{a}\boldsymbol{a}^{\mathrm{H}} \right) \sin(\theta)\, d\theta && (11) \\ &= \frac{1}{2} \left(\boldsymbol{a}_{\mathrm{imp}}^* \boldsymbol{a}_{\mathrm{imp}}^{\mathrm{T}} \odot \int_{-\pi/2}^{\pi/2} \boldsymbol{a}\boldsymbol{a}^{\mathrm{H}} \sin(\theta)\, d\theta \right) && (12) \\ &= \frac{1}{2} \left(\boldsymbol{a}_{\mathrm{imp}}^* \boldsymbol{a}_{\mathrm{imp}}^{\mathrm{T}} \odot \boldsymbol{R} \right). && (13) \end{aligned}$$

The elements of the matrix $\boldsymbol{R} = \int_{-\pi/2}^{\pi/2} \boldsymbol{a}\boldsymbol{a}^{\mathrm{H}} \sin(\theta)\, d\theta$ can be evaluated in a closed form [16]. To this end, the (m, n)-th element can be written as

$$\left[\boldsymbol{R}\right]_{m,n} = 2\,\mathrm{si}\left(\frac{2\pi}{\lambda} \left\|\boldsymbol{p}_m - \boldsymbol{p}_n\right\|\right), \qquad (14)$$

where $\boldsymbol{p}_m$ and $\boldsymbol{p}_n$ are the coordinate vectors of the m-th and n-th elements, correspondingly, and $\mathrm{si}(x) = \frac{\sin(x)}{x}$.

Conventional methods for robust beamforming [17–19] assume the availability of the covariance matrix or signal snapshots during the adaptation process. Unfortunately, for an RIS the situation differs. An RIS is a passive device and any measurements might be conducted only indirectly and are usually associated with high signalling overheads. This motivates us to look for new methods that do not need such information. A similar problem is solved in the field of antenna beam pattern synthesis where the desired beamforming coefficients are computed based on the antenna model and the coordinates of the sensors. Convex optimization methods can also be applied to solve this class of problems [15, 20].

In this paper, we maximize the directivity of the RLA subject to constant modulus constraints (CMCs)

$$\begin{aligned} \text{(P1):} \quad & \underset{\boldsymbol{\phi}}{\text{maximize}} \quad D\left(\theta; \theta_{\mathrm{tx}}, \boldsymbol{\phi}\right) && (15a) \\ & |\phi_i| = 1, \;\; 0 \leq \arg(\phi_i) \leq 2\pi, && (15b) \\ & \forall i \in \left[\, 0 \,..\, N_{\mathrm{cell}} - 1 \,\right]. \end{aligned}$$

However, the corresponding optimization problem is non-convex [15], therefore we propose to consider the following convex relaxation

$$\begin{aligned} \text{(P2):} \quad & \underset{\boldsymbol{\phi}}{\text{minimize}} \quad \boldsymbol{\phi}^{\mathrm{H}} \boldsymbol{B}(\theta_{\mathrm{tx}}) \boldsymbol{\phi} && (16a) \\ & \text{subject to} \quad \boldsymbol{\phi}^{\mathrm{H}} \boldsymbol{A}(\theta; \theta_{\mathrm{tx}}) \boldsymbol{\phi} = 1, && (16b) \end{aligned}$$

which is equivalent to (15a). After we find a solution for (P2) we perform aperture thinning [21] that is based on the randomization technique in order to satisfy the CMCs.

2.3. Impact of thermal deformations

We assume that the parameters experience fluctuations due to thermal deformations, even though we know the coordinates of the phase centers for the transmitter, the RLA, and the receiver perfectly.

We assume that the thermal deformations lead to displacement $\boldsymbol{\Delta}_{p,n} \in \mathbb{R}^2$, $n \in [\,0, N_{\text{cell}} - 1\,]$ in (x, y) coordinates of every element of the RLA. We use the deterministic uncertainty region model in which the error is bounded, i.e., $\|\boldsymbol{\Delta}_{p,n}\|_2 \leq \sigma$. We assume that different coordinates are uncorrelated, while the maximum perturbation is known. Also we assume identical bounds in x and y directions, i.e., $\sigma_{\text{x}} = \sigma_{\text{y}} = \sigma$. Hence, he actual position of a sensor belongs to the set

$$\mathcal{P}(\sigma) \triangleq \left\{\, \tilde{\boldsymbol{p}} \mid \tilde{\boldsymbol{p}} = \boldsymbol{p} + \boldsymbol{p}_{\text{err}},\ \|\boldsymbol{p}_{\text{err}}\| \leq \sigma \,\right\}. \tag{17}$$

As a result, the deflection of the RLA causes additional phase shifts common for impinging and reflected steering vectors. Further, we show that the thermal deformations have an impact not only on the impinging $\boldsymbol{a}_{\text{imp}}$ and the reflected $\boldsymbol{a}_{\text{rfl}}$ steering vectors but also on the matrix $\boldsymbol{B}(\theta_{\text{tx}})$. We present, in this paper, how to design the robust reflective beamforming for an RLA based on the knowledge of the bound σ on the norm of the displacement $\boldsymbol{p}_{\text{err}}$.

Next, we describe how to find the bound on the error of the n-th element of the compound vector $\boldsymbol{a}_{\text{c}} = \boldsymbol{a}^*_{\text{imp}} \odot \boldsymbol{a}$ and then generalize the result on the norm for the perturbation of the whole vector. First, we compute the first-order Taylor expansion which is a valid approximation for small perturbations.

$$\begin{aligned} \mathrm{e}^{j\left(\,\alpha_n + \alpha_{n,\text{err}}\,\right)} &= \mathrm{e}^{j\alpha_n} + j\alpha_{n,\text{err}}\mathrm{e}^{j\alpha_n} + \mathcal{O}\left(\alpha^2_{n,\text{err}}\right) & (18)\\ &\approx \mathrm{e}^{j\alpha_n} + \mathit{\Delta}_{\alpha,n}, & (19) \end{aligned}$$

where $\mathit{\Delta}_{\alpha,n} = j\,\alpha_{n,\text{err}}\,\mathrm{e}^{j\alpha_n}$. Thus it can be shown that the norm of the perturbation is equal to $\|\mathit{\Delta}_{\alpha,n}\| = |\alpha_{n,\text{err}}|$.

In our work we assume that $\alpha_n = -\frac{2\pi}{\lambda}\boldsymbol{p}^{\text{T}}_n\boldsymbol{u}$, where $\boldsymbol{p} = [\,p_n, 0\,]^{\text{T}} \in \mathbb{R}^2$ is the vector of coordinates of the n-th element of the RLA and $\boldsymbol{u} = [\,\sin(\theta), \cos(\theta)\,]^{\text{T}} \in \mathbb{R}^2$. Then the perturbed value $\tilde{\alpha}_n$ can be written as

$$\tilde{\alpha}_n = -\frac{2\pi}{\lambda}\left(\,\boldsymbol{p}_n + \boldsymbol{p}_{\text{err},n}\,\right)^{\text{T}}\boldsymbol{u} = -\frac{2\pi}{\lambda}\boldsymbol{p}^{\text{T}}_n\boldsymbol{u} - \frac{2\pi}{\lambda}\boldsymbol{p}^{\text{T}}_{\text{err},n}\boldsymbol{u}, \tag{20}$$

where we can write $\alpha_{n,\text{err}} = -\frac{2\pi}{\lambda}\boldsymbol{p}^{\text{T}}_{\text{err},n}\boldsymbol{u}$. Based on this result, we can conclude that the value of $\alpha_{n,\text{err}}$ can be bounded by an ellipsoid of the form

$$\mathcal{E} = \left\{\, \frac{2\pi}{\lambda}\boldsymbol{u}^{\text{T}}\boldsymbol{p}_{\text{err},n} \mid \|\boldsymbol{p}_{\text{err},n}\| \leq \sigma \,\right\}. \tag{21}$$

However, in this paper, we consider the worst-case bound, which can be written as $\boldsymbol{p}^{\text{T}}_{\text{err},n}\boldsymbol{u} \leq \sqrt{2}\sigma$, taking into account that $|\cos(\theta) + \sin(\theta)| \leq \sqrt{2}$. As a result, the bound on the perturbation of the n-th element of the RLA can be found as $\|\mathit{\Delta}_{\alpha,n}\| \leq \frac{2\sqrt{2}\pi}{\lambda}\sigma$. Consequently, for the whole steering vector, the bound on the worst-case perturbation can be found as the geometrical mean of bounds for the individual elements

$$\|\mathit{\Delta}\boldsymbol{a}_{\text{c}}\| = \sqrt{\sum_{n=1}^{N_{\text{cell}}} \mathit{\Delta}^2_{\alpha,n}} \leq \frac{2\sqrt{2}\pi}{\lambda}\sqrt{N_{\text{cell}}}\sigma = \gamma. \tag{22}$$

The expression (22) represents the worst-case bound on the norm perturbation of the steering vector due to the sensor position displacement caused by thermal deformations.

For the second step, we derive the bound on the perturbation of the matrix $\boldsymbol{B}(\theta_{\text{tx}})$. The (m, n)-th element of the matrix can be written as

$$\Big[\,\boldsymbol{B}(\theta_{\text{tx}})\,\Big]_{m,n} = \mathrm{e}^{j\frac{2\pi}{\lambda}\mathit{\Delta}\boldsymbol{p}^{\text{T}}_{mn}\boldsymbol{u}} \cdot \mathrm{si}\left(\frac{2\pi}{\lambda}\|\mathit{\Delta}\boldsymbol{p}_{mn}\|\right), \tag{23}$$

where $\mathit{\Delta}\boldsymbol{p}_{mn} = \boldsymbol{p}_m - \boldsymbol{p}_n$. We ignore the variations in phase for the elements of the matrix $\boldsymbol{B}$ in the expression (23) and focus only on the second term which represents the amplitude. The derivative of the si () function can be written as

$$\frac{\partial\,\mathrm{si}\,(\alpha x)}{\partial x} = \frac{\cos(\alpha x) - \mathrm{si}\,(\alpha x)}{x}. \tag{24}$$

Note that in a neighborhood of x, the derivative gives us local information about the direction of increase of the target function.

Let us denote the perturbed difference in distance between the (m, n) pair of the RLA elements as $\mathit{\Delta}\tilde{\boldsymbol{p}}_{mn} = \mathit{\Delta}\boldsymbol{p}_{mn} + \boldsymbol{e}_{mn}$. Then we can write the expression (25) for the worst case perturbation of the (m, n) element of the matrix $\boldsymbol{B}$. We also assume that the norm on the perturbation can be replaced by its bound, i.e., $\|\boldsymbol{e}_{mn}\| = 2\sigma$.

Then the bound on the perturbation of the matrix $\boldsymbol{B}$ can be found similarly as for the perturbation of the steering vector via the geometric mean of the bounds for all elements of the matrix

$$\|\mathit{\Delta}\boldsymbol{B}\|_{\text{F}} = 2\sigma\sqrt{\sum_{m=0}^{N_{\text{cell}}}\sum_{n=0}^{N_{\text{cell}}}\Big[\,\mathit{\Delta}\boldsymbol{B}\,\Big]^2_{m,n}} = \eta, \tag{26}$$

where

$$\Big[\,\mathit{\Delta}\boldsymbol{B}\,\Big]_{m,n} = \frac{\cos\left(\frac{2\pi}{\lambda}\|\mathit{\Delta}\boldsymbol{p}_{mn}\|\right) - \mathrm{si}\left(\frac{2\pi}{\lambda}\|\mathit{\Delta}\boldsymbol{p}_{mn}\|\right)}{\|\mathit{\Delta}\boldsymbol{p}_{mn}\|}. \tag{27}$$

As a result, we can calculate the worst-case bound η on the perturbation of the matrix $\boldsymbol{B}$ caused by thermal deformation of the geometry of the RLA.

3. ROBUST REFLECTIVE BEAMFORMING

The material in the section follows mainly the derivations in [17,22] and we refer the interested readers to these publications for more details.

According to our system model, the compounding vector $\boldsymbol{a}_{\text{c}}$ and the matrix $\boldsymbol{B}$ are known imprecisely, i.e., contain uncertainties. They can be written as

$$\tilde{\boldsymbol{a}}_{\text{c}} = \boldsymbol{a}_{\text{c}} + \mathit{\Delta}\boldsymbol{a} \quad \text{and} \quad \tilde{\boldsymbol{B}} = \boldsymbol{B} + \mathit{\Delta}\boldsymbol{B}. \tag{28}$$

in terms of perfect values and unknown perturbations. However, we assume that these perturbations are caused by thermal deformations of the geometry of the RLA and thus can be bounded assuming the bound on the displacement of each element, i.e.,

$$\|\mathit{\Delta}\boldsymbol{a}\| \leq \gamma \quad \text{and} \quad \|\mathit{\Delta}\boldsymbol{B}\|_{\text{F}} \leq \eta. \tag{29}$$

The expressions (22) and (26) represent the bounds on the norms of the perturbation of the compounding steering vector and the corresponding matrix as a function of the bound on the displacement, respectively.

In this subsection, we describe the solution for the robust reflective beamforming for the RLA that takes into account the derived bounds.

$$\mathrm{si}\left(\frac{2\pi}{\lambda}\|\boldsymbol{\Delta}\tilde{\boldsymbol{p}}_{mn}\|\right) \approx \mathrm{si}\left(\frac{2\pi}{\lambda}(\|\boldsymbol{\Delta}\boldsymbol{p}_{mn}\| + \|\boldsymbol{e}_{mn}\|)\right) \leq \mathrm{si}\left(\frac{2\pi}{\lambda}\|\boldsymbol{\Delta}\boldsymbol{p}_{mn}\|\right) + \frac{\cos\left(\frac{2\pi}{\lambda}\|\boldsymbol{\Delta}\boldsymbol{p}_{mn}\|\right) - \mathrm{si}\left(\frac{2\pi}{\lambda}\|\boldsymbol{\Delta}\boldsymbol{p}_{mn}\|\right)}{\|\boldsymbol{\Delta}\boldsymbol{p}_{mn}\|}\|\boldsymbol{e}_{mn}\| \tag{25}$$

The updated optimization problem can be written as

$$\text{(P3):} \quad \min_{\boldsymbol{\phi}} \max_{\|\boldsymbol{\Delta B}\| \leq \eta} \quad \boldsymbol{\phi}^{\mathrm{H}}(\boldsymbol{B} + \boldsymbol{\Delta B})\boldsymbol{\phi} \tag{30a}$$

$$\text{subject to} \quad (\boldsymbol{a}_{\mathrm{c}} + \boldsymbol{\Delta a})^{\mathrm{H}}\boldsymbol{\phi} = 1, \forall \|\boldsymbol{\Delta a}\| \leq \gamma. \tag{30b}$$

It can be shown [17,22,23] that the aforementioned optimization problem can be relaxed and written in the following form[1]

$$\text{(P4):} \quad \underset{\boldsymbol{\phi}}{\text{minimize}} \quad \boldsymbol{\phi}^{\mathrm{H}}(\boldsymbol{B} + \eta \boldsymbol{I})\boldsymbol{\phi} \tag{31a}$$

$$\text{subject to} \quad \mathrm{Re}\left(\boldsymbol{a}_{\mathrm{c}}^{\mathrm{H}}\boldsymbol{\phi}\right) \geq 1 + \gamma\|\boldsymbol{\phi}\|, \tag{31b}$$

$$\mathrm{Im}\left(\boldsymbol{a}_{\mathrm{c}}^{\mathrm{H}}\boldsymbol{\phi}\right) = 0, \tag{31c}$$

where η and γ can be calculated using the expressions (22) and (26). The presented optimization problem (P4) can be solved by available solvers for convex programming. For example, it can be written in the form of a Second Order Cone Program (SOCP) and be solved via a primal-dual interior point method with the complexity $\mathcal{O}\left(N_{\mathrm{cell}}^{3}\right)$.

However, practical designs require additional constraints (15b) for constant modulus on weight coefficients, that were excluded from (P4). In order to account for the constraint (15b) we propose an ad hoc solution, namely, to implement an additional stage for thinning of the RLA in order to imitate variation of the amplitude across the aperture by changing the density of the elements [21]. Such a thinning operation might be performed during the design stage or by accounting for the possibility to turn the cell elements into the absorption mode.

4. SIMULATION RESULTS

In this section, we present the selected simulation results to demonstrate the performance of the proposed robust reflective beamforming for non-terrestrial networks under thermal deformations.

For the simulation setup we consider the RLA with $N_{\mathrm{cell}} = 32$ and spacing $\Delta = \frac{\lambda}{5}$. For the presented results, we ignore the path loss and consider the worst case directivity as the metric of the performance. The worst-case directivity is calculated as

$$D_{\mathrm{wc}} = \frac{\left|(\,\boldsymbol{a}_{\mathrm{c}}(\theta_{\mathrm{rx}}, \theta_{\mathrm{tx}}) + \boldsymbol{e}\,)^{\mathrm{H}}\,\boldsymbol{\phi}\right|^{2}}{\boldsymbol{\phi}^{\mathrm{H}}(\boldsymbol{B} + \eta\boldsymbol{I})\boldsymbol{\phi}}, \text{ where } \boldsymbol{e} = -\gamma\frac{\boldsymbol{w}}{\|\boldsymbol{w}\|}\mathrm{e}^{j\angle\boldsymbol{\phi}^{\mathrm{H}}\boldsymbol{a}}. \tag{32}$$

During the thinning operation we evaluate 1000 random sequences of indices and choose the one with the largest achieved directivity. For the first reference algorithms we consider the expression (4), which is used to calculate the reflection coefficients as the difference in phase between the impinging and the reflected waves. For the second algorithm we consider worst-case beamforming based on [17] accounting for the perturbations of the steering vectors.

In Fig. 1 we can observe that the proposed solution has a better performance in terms of the directivity in comparison to non-optimized and partially optimized solutions. The continues line correspond to a solution after thinning, the dashed lines correspond to solutions prior to thinning.

[1] We omit the detailed derivation due to the restriction on space for the conference version of the paper.

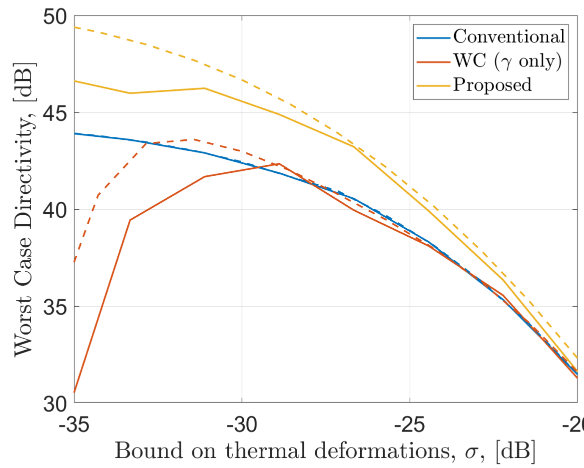

Fig. 1. The performance of the proposed robust reflective beamforming. The dashed lines relates to the solutions before thinning. The solid lines are obtained by applying the thinning procedure to the solution of the corresponding convex programs.

5. CONCLUSIONS AND FUTURE DIRECTIONS

In this paper, we present a method for robust reflective beamforming for non-terrestrial communications. We analytically derive the bounds on the perturbations of the covariance matrix and the steering vectors as functions of the coordinate displacement of the elements of the reflective geometry. The presented simulation results confirm the derivations and show the performance of the beamforming under worst case perturbations. These results show the possibility of designing better space antenna systems that are able to provide direct connectivity to existing mobile terminals on Earth and provide cellular access to the internet to sparsely populated rural areas of the world.

The results of this paper open several directions for future research. These include a modification of the presented bounds to better represent the model through ellipsoidal uncertainty regions. This might be necessary if the maximum bound along different axes vary. Moreover, an extension of the uncertainty region to three dimensions is also relevant. We can also extend the presented results to the case of two-dimensional or distributed reflective structures.

Furthermore, an extension to multi-user scenarios, i.e., the RIS-assisted broadcast channel, can be considered. In this case, the directivity is replaced by the SINR in the objective function. The thermal deformation model is used, and a similar optimization model can be derived. Of particular interest is also an extension of the described worst-case beamforming and a derivation of the corresponding bounds for the near-field regime of operation, when one or both sides of the communications link are within the near-field region of an RLA or an RIS.

6. REFERENCES

[1] M. D. Renzo, M. Debbah, D.-T. Phan-Huy, A. Zappone, M.-S. Alouini, C. Yuen, V. Sciancalepore, G. C. Alexandropoulos, J. Hoydis, H. Gacanin, J. de Rosny, A. Bounceur, G. Lerosey, and M. Fink, "Smart radio environments empowered by reconfigurable AI meta-surfaces: An idea whose time has come," *EURASIP Journal on Wireless Communications and Networking*, vol. 2019, no. 1, p. 129, May 2019.

[2] Q. Wu and R. Zhang, "Intelligent Reflecting Surface Enhanced Wireless Network via Joint Active and Passive Beamforming," *IEEE Transactions on Wireless Communications*, vol. 18, no. 11, pp. 5394–5409, 2019.

[3] K. Tekbıyık, G. K. Kurt, A. R. Ekti, and H. Yanikomeroglu, "Reconfigurable Intelligent Surfaces in Action for Nonterrestrial Networks," *IEEE Vehicular Technology Magazine*, vol. 17, no. 3, pp. 45–53, Sep. 2022.

[4] J. Ye, J. Qiao, A. Kammoun, and M.-S. Alouini, "Nonterrestrial Communications Assisted by Reconfigurable Intelligent Surfaces," *Proceedings of the IEEE*, vol. 110, no. 9, pp. 1423–1465, Sep. 2022.

[5] W. U. Khan, E. Lagunas, A. Mahmood, B. M. ElHalawany, S. Chatzinotas, and B. Ottersten, "When RIS Meets GEO Satellite Communications: A New Sustainable Optimization Framework in 6G," in *Proc. 95th Vehicular Technology Conference (VTC2022-Spring)*, Jun. 2022, pp. 1–6.

[6] Z. Lin, H. Niu, K. An, Y. Wang, G. Zheng, S. Chatzinotas, and Y. Hu, "Refracting RIS Aided Hybrid Satellite-Terrestrial Relay Networks: Joint Beamforming Design and Optimization," *IEEE Transactions on Aerospace and Electronic Systems*, pp. 1–1, 2022.

[7] R. Sharp, M. Liao, J. Giriunas, J. Heighway, A. Lagin, and R. Steinbach, "Reflector surface distortion analysis techniques (thermal distortion analysis of antennas in space)," Jul. 1989. [Online]. Available: https://ntrs.nasa.gov/citations/19900009951

[8] Y. Rahmat-Samii, "Effects of deterministic surface distortions on reflector antenna performance," *Annales Des Télécommunications*, vol. 40, no. 7, pp. 350–360, Jul. 1985.

[9] C. A. Balanis, *Antenna Theory: Analysis and Design*, 4th ed. Wiley, 2016.

[10] E. Björnson and L. Sanguinetti, "Power Scaling Laws and Near-Field Behaviors of Massive MIMO and Intelligent Reflecting Surfaces," *IEEE Open Journal of the Communications Society*, vol. 1, pp. 1306–1324, 2020.

[11] E. Björnson, Ö. T. Demir, and L. Sanguinetti, "A Primer on Near-Field Beamforming for Arrays and Reconfigurable Intelligent Surfaces," in *Proc. 55th Asilomar Conference on Signals, Systems, and Computers*, Oct. 2021, pp. 105–112.

[12] L. Laursen, "No More "No Service": Cellphones will increasingly text via satellite," *IEEE Spectrum*, vol. 60, no. 1, pp. 52–55, Jan. 2023.

[13] E. Björnson, H. Wymeersch, B. Matthiesen, P. Popovski, L. Sanguinetti, and E. de Carvalho, "Reconfigurable Intelligent Surfaces: A Signal Processing Perspective With Wireless Applications," *IEEE Signal Processing Magazine*, vol. 39, no. 2, pp. 135–158, Mar. 2022.

[14] E. Basar, M. Di Renzo, J. De Rosny, M. Debbah, M.-S. Alouini, and R. Zhang, "Wireless Communications Through Reconfigurable Intelligent Surfaces," *IEEE Access*, vol. 7, pp. 116 753–116 773, 2019.

[15] Y.-X. Zhang, Y.-C. Jiao, and L. Zhang, "Antenna Array Directivity Maximization With Sidelobe Level Constraints Using Convex Optimization," *IEEE Transactions on Antennas and Propagation*, vol. 69, no. 4, pp. 2041–2052, Apr. 2021.

[16] H. L. Van Trees, *Optimum Array Processing*. John Wiley & Sons, Inc., Mar. 2002.

[17] S. Vorobyov, A. Gershman, and Z.-Q. Luo, "Robust adaptive beamforming using worst-case performance optimization: A solution to the signal mismatch problem," *IEEE Transactions on Signal Processing*, vol. 51, no. 2, pp. 313–324, Feb. 2003.

[18] J. Li, P. Stoica, and Z. Wang, "On robust Capon beamforming and diagonal loading," *IEEE Transactions on Signal Processing*, vol. 51, no. 7, pp. 1702–1715, Jul. 2003.

[19] R. Lorenz and S. Boyd, "Robust minimum variance beamforming," *IEEE Transactions on Signal Processing*, vol. 53, no. 5, pp. 1684–1696, May 2005.

[20] H. Lebret and S. Boyd, "Antenna array pattern synthesis via convex optimization," *IEEE Transactions on Signal Processing*, vol. 45, no. 3, pp. 526–532, Mar. 1997.

[21] R. J. Mailloux, *Phased Array Antenna Handbook*, 3rd ed. Artech House, Nov. 2017.

[22] S. Vorobyov, A. Gershman, Z.-Q. Luo, and N. Ma, "Adaptive beamforming with joint robustness against mismatched signal steering vector and interference nonstationarity," *IEEE Signal Processing Letters*, vol. 11, no. 2, pp. 108–111, Feb. 2004.

[23] S. Shahbazpanahi, A. Gershman, Z.-Q. Luo, and K. M. Wong, "Robust adaptive beamforming for general-rank signal models," *IEEE Transactions on Signal Processing*, vol. 51, no. 9, pp. 2257–2269, Sep. 2003.